

*An analysis of the method for ensuring the sinusoidality of the output voltage in power generation systems with self-commutated voltage inverters under the requirements of the international standard IEEE-519 is presented.*

*In a number of programs, especially low-power generation systems, a low-cost solution is needed to provide the sinusoidal waveform of the output voltage with the total harmonic distortion of 5 %. This solution is to use two-level voltage inverters with an output sine LC filter. However, the feature of the sine filter with the frequency converter is that the PWM frequency affects the spectrum of higher harmonics of the output voltage. In addition, there is the starting current of the filter capacitor, which can disable the power switches of the voltage inverter.*

*The developed method for calculating the values of the LC filter with the two-level voltage inverter in the PWM mode is presented meeting the requirements of the international standard IEEE-519, taking into account the modulation frequency and limitation of the starting current of the filter capacitor.*

*To confirm the required quality of the output voltage of the two-level voltage inverter with the sine filter, an appropriate simulation model was created in the Matlab/Simulink computer simulation environment. The oscillograms and harmonic analysis of the input and output voltages of the sine filter, which showed the total harmonic distortion of 1.88 %, are presented.*

*A physical prototype of the investigated system was created on the basis of a 5.5 kW OVEN PChV203-5K5-V frequency converter (Ukraine). Using the SIGLENT SDS1104X-E oscilloscope (China), the real waveform and the results of the harmonic analysis of the sine filter output voltage, confirming the implementation of the necessary sinusoidality criteria, were obtained*

*Keywords: self-commutated voltage inverter, power quality, total harmonic distortion, sine filter, power sources*

UDC 621.314

DOI: 10.15587/1729-4061.2021.225327

# A METHOD FOR CALCULATING THE PARAMETERS OF THE SINE FILTER OF THE FREQUENCY CONVERTER, TAKING INTO ACCOUNT THE CRITERION OF STARTING CURRENT LIMITATION AND PULSE-WIDTH MODULATION FREQUENCY

**V. Nerubatskyi**

PhD, Associate Professor\*

E-mail: NVP9@i.ua

**O. Plakhtii**

PhD, Electronic Engineer

Limited Liability Company «VO OVEN»

Hvardiytsiv-Shyronivtsiv str., 3A, Kharkiv, Ukraine, 61153

E-mail: a.plakhtiy1989@gmail.com

**D. Hordiienko**

Postgraduate Student\*

E-mail: D.Hordiienko@i.ua

**S. Mykhalkiv**

PhD, Associate Professor

Department of Maintenance and Repair of Rolling Stock\*\*

E-mail: svm\_m@ukr.net

**V. Ravluyk**

PhD, Associate Professor

Department of Wagons\*\*

E-mail: ravvg@ukr.net

\*Department of Electrical Power Engineering, Electrical Engineering and Electromechanics\*\*

\*\*Ukrainian State University of Railway Transport  
Feierbakha sq., 7, Kharkiv, Ukraine, 61050

Received date 02.12.2020

Accepted date 25.01.2021

Published date 26.02.2021

Copyright © 2021, V. Nerubatskyi, O. Plakhtii, D. Hordiienko, S. Mykhalkiv, V. Ravluyk

This is an open access article under the CC BY license

(<http://creativecommons.org/licenses/by/4.0>)

## 1. Introduction

The share of alternative power sources in the overall energy sector is growing every year. According to the UN, in 2008, \$190 billion was invested in alternative power proj-

ects worldwide, while \$110 billion was invested in coal and oil production [1, 2].

In 2018, global investments in clean energy totaled \$332.1 billion, the bulk of which falls on solar, wind, geothermal and bioenergy (Fig. 1) [3, 4].

According to the British Petroleum (BP) transnational oil and gas company, in 2019 the share of alternative renewable energy sources (excluding large hydropower plants) was 10.4 % in global power generation, surpassing nuclear energy for the first time. In primary energy (total energy balance), the share of alternative energy increased to 5 %, rising from 4.5 % in 2018 and also bypassing nuclear energy [5, 6].

As of 2017, alternative energy sources generated 9.6 % of electricity in the United States, including 6.3 % from wind and 1.3 % from solar power plants. Taking into account large hydropower plants, the contribution of renewable energy sources amounted to 17.1 % of electricity produced in the United States [7].

In the first half of 2020, renewable energy sources in Germany produced a record 56 % of electricity. Of these, 4 % were generated by traditional hydroelectric power and 52 % by alternative sources. Wind ranked first among power sources, generating 30.6 % of electricity, and the sun gave 11.4 %.

Self-commutated voltage inverters are among the most widely used in the industry, as well as in the transport of semiconductor power converters [8]. In cases where self-commutated voltage inverters are used in power supply and control systems for asynchronous and synchronous electric drives, the quality, namely harmonic composition, of the output voltage is not critical. That is why the engine torque is provided by the sinusoidal waveform of the output current [9, 10]. At the same time, in a number of technical programs, the quality of the output voltage of self-commutated voltage inverters is a critical parameter. Examples of self-commutated voltage inverters are converters in renewable and alternative power generation systems. An example of such a system is shown in Fig. 2 [11].

The task of power semiconductor converters operating with alternative energy sources is to generate power to the general industrial network or to create an autonomous power supply system. The basic requirements for the quality of power generated by voltage inverters are regulated by international standards.

Requirements for the allowable voltage total harmonic distortion  $THD_U$  in general industrial electrical networks under the international standard IEEE-519 are given in Table 1.

$THD_U$  is defined according to the expression [12]:

$$THD_U = \frac{\sqrt{\sum_{h=2}^{\infty} U_h^2}}{U_1} \tag{1}$$

The most common circuit implementing DC-to-AC conversion is a two-level self-commutated voltage inverter. The value of the total harmonic distortion of the output

voltage of the two-level voltage inverter is 65...70 %, which does not meet the voltage quality requirements under the international standard IEEE-519. Therefore, special technical solutions are used to ensure the high quality of the inverter output voltage, such as various multilevel voltage inverter circuits. So, cascaded multilevel inverters, modular multilevel inverters, diode-clamped multilevel inverters, flying-capacitor multilevel inverters and other circuits are used [13, 14]. It should be noted that there are problems in ensuring electromagnetic compatibility in the mode of power generation in the general industrial network and in the mode of creating an autonomous power source.

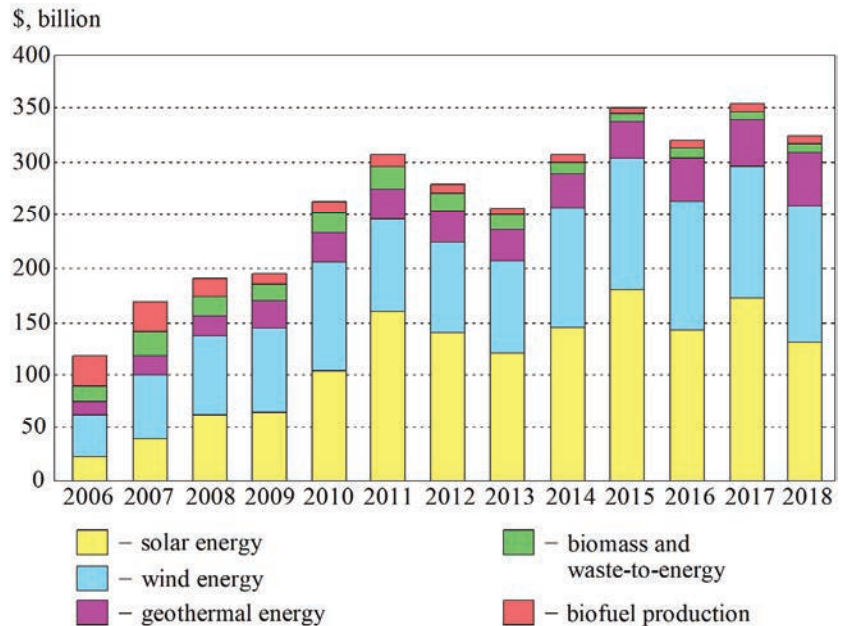


Fig. 1. Investments in renewable energy from 2006 to 2018

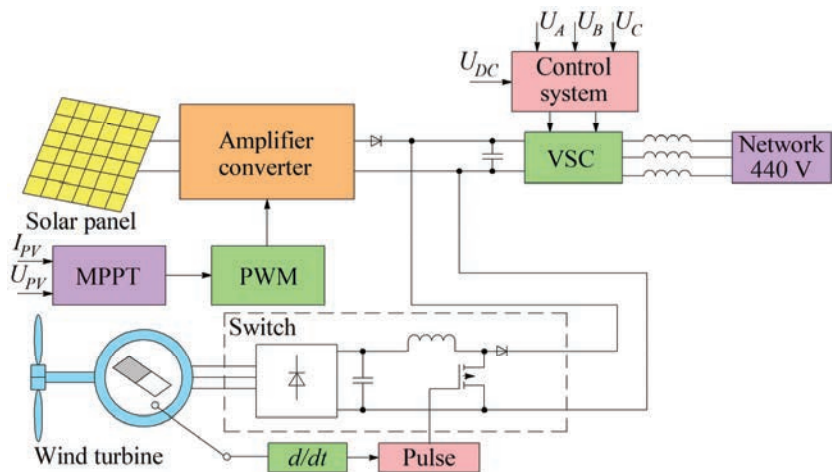


Fig. 2. Block diagram of the integrated “wind turbine – solar panel – general industrial network” system

Table 1

Voltage harmonic distortion limits		
Voltage	$U_b$ (%)	$THD_U$ (%)
$U < 69$ kV	3.0	5.0
$69 \text{ kV} \leq U < 161$ kV	1.5	2.5
$U \geq 161$ kV	1.0	1.5

**2. Literature review and problem statement as to forming the sinusoidal waveform of the output voltage of self-commutated inverters**

The typical waveform of the output voltage of various types of multilevel inverters is common (Fig. 3). The number of levels in the output voltage and, accordingly, waveform sinusoidality depend on the number of levels in the power circuit of multilevel voltage inverters and the number of power elements of the circuit, and hence the cost.

The dependence of the total harmonic distortion  $THD_U$  of multilevel inverters on the number of levels  $N_l$  obtained during the study is given in Fig. 4.

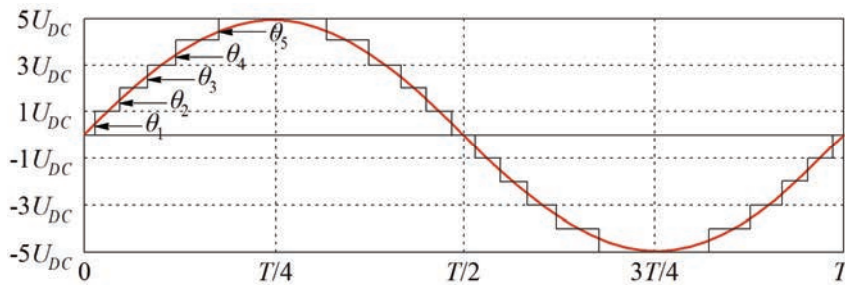


Fig. 3. Typical waveform of the output voltage of the multilevel inverter in the single-modulation mode

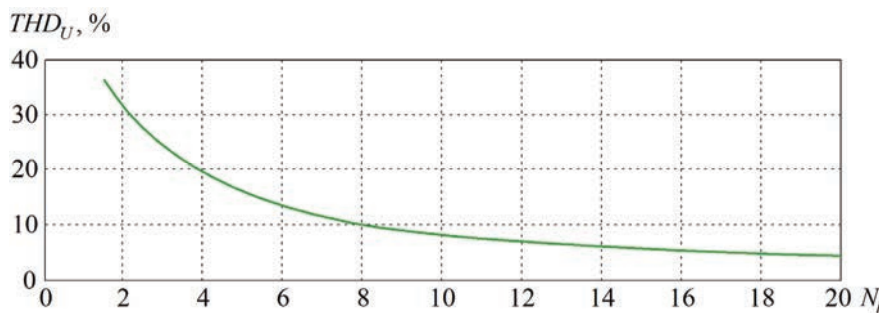


Fig. 4. Dependence of total harmonic distortion on the number of levels

As can be seen from Fig. 4, to ensure the total harmonic distortion of the output voltage of the multilevel inverter below 5 %, the number of levels in the multilevel inverter must exceed 20.

In [15, 16], studies of the output voltage quality of cascaded multilevel voltage inverters are given. The disadvantage of cascaded voltage inverters is the need for a large number of galvanically isolated DC sources. In addition, the implementation of this circuit requires an increased number of power transistors [17, 18], which increases the cost of this system.

In [19, 20], the research of the output voltage quality of modular multilevel voltage inverters is given. The disadvantage of modular voltage inverters is the need for a fairly complex algorithm for voltage stabilization on cell capacitors. In addition, the implementation of this circuit requires an increased number of power transistors and high-capacity capacitors [21, 22], which also increases the cost of this system.

In [23, 24], diode-clamped inverter circuits are considered, which require an increased number of power transistors, capacitors and diodes, which leads to a significant increase in the cost of this circuit solution.

In addition to circuit solutions related to the implementation of a high number of output voltage levels of inverters [25, 26], there are algorithmic methods to improve the sinusoidality of the output voltage. One such method is the implementation of the overmodulation [27] and waveform optimum [28] mode.

In [29], the study of improving the quality of the output voltage in two-level self-commutated voltage inverters in the overmodulation mode is presented. The study showed that the overmodulation mode for the two-level inverter can reduce the total harmonic distortion of the output voltage of the two-level inverter from 68 % to 32 % (Fig. 5). The advantage of this solution is a fairly significant improvement in

the waveform of the output voltage in multi-level inverters. Despite a significant improvement in the sinusoidality of the output voltage of the SCVI in the overmodulation mode, its  $THD$  remains unsatisfactory to the requirements of the IEEE-519 standard.

It is possible to ensure high-quality output voltage of two-level inverters by using output sine filters. The advantage of this solution is the ability to ensure high-quality output voltage with minimum economic costs. At the same time, the disadvantage of this solution is the starting current mode of sine filters, which can cause breakdowns of the inverter power switches, or in the presence of hardware protection, it can enter the protection mode.

In [30, 31], the study of improving the output voltage waveform of two-level voltage inverters using output sine filters is presented. However, the works do not provide a study of sinusoidality of the output voltage of the inverter with the

sine filter, do not define the method of calculating the components taking into account the requirements for ensuring the total harmonic distortion of 5 %. In addition, no study of the starting currents of the sine filter is given.

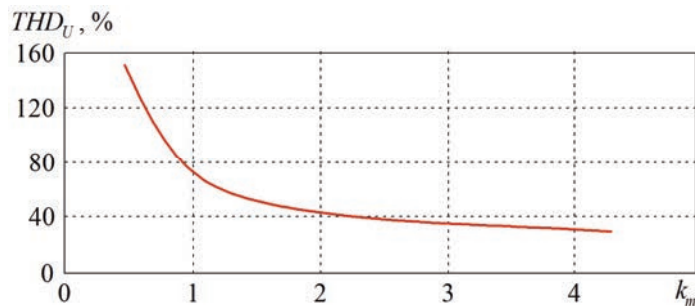


Fig. 5. Dependence of total harmonic distortion  $THD_U$  on modulation coefficient  $k_m$

In [32], the mathematical model of the attitude matrix of the sine filter with the frequency converter is given. The disadvantage of the study is the lack of methods for determining the filter parameters, as well as the lack of a study of the starting current of the filter capacitor.

In [33], the research of the LCL filter of the self-commutated voltage inverter and active voltage rectifier is given. The disadvantage of the study is the lack of methods for determining the filter parameters, the lack of analysis of voltage sinusoidality, as well as the lack of a study of the filter capacitor starting current.

In [34], the method of designing three-phase frequency converter LC filters is given. The disadvantage is the lack of research on the sinusoidality of the LC filter output voltage. In addition, no study of the starting currents of the sine filter capacitors is given.

Thus, from this review we can conclude that the issue of creating a method for calculating the values of sine filters of self-commutated voltage inverters taking into account the pulse-width modulation frequency of the inverter and the requirement of starting current limitation is unresolved. In this case, the requirements of voltage sinusoidality  $THD_U < 5\%$  should be met under the international standard IEEE-519.

### 3. The aim and objectives of the study

The aim of the study is to create a method for calculating the values of the sine filter of the self-commutated voltage inverter, which takes into account the pulse-width modulation frequency of the inverter and allows the limitation of the filter capacitor starting current.

To achieve the aim, the following objectives were set:

- to create analytical dependences of the values of the sine filter with the two-level voltage inverter taking into account the PWM frequency of the inverter to ensure the quality requirements of the output voltage according to the international standard IEEE-519 taking into account the limitations of filter values by the criterion of the maximum inverter starting current;
- to confirm the reliability of the created analytical dependences by computer simulation of the three-phase two-level voltage inverter with the developed output sine filter in the Matlab 2017b software environment, as well as to study the output voltage of the sine filter;
- to confirm the reliability of the created analytical dependences of sine filter values to ensure the sinusoidal waveform of the sine filter output voltage on the physical stand based on the PChV203-5K5-V frequency converter, as well as to study the harmonic spectrum of the sine filter output voltage.

### 4. Materials and methods of the study

The study was carried out using the basic laws of electrical engineering, computer simulation of semiconductor power converters, mathematical apparatus of fast Fourier transform and physical prototyping of the studied system.

The results were confirmed by computer experiments on simulation models and physical experiments on the developed bench.

### 5. Analytical dependences of the values of the sine filter with two-level voltage inverter

Generation of sinusoidal voltage requires a clear understanding of the magnitude and order of harmonics that need to be reduced, namely, voltage inverter harmonics [35, 36].

Fig. 6 shows the diagram of the two-level three-phase self-commutated voltage inverter with the sine filter.

The typical waveform and harmonic spectrum of the output phase voltage of the three-phase PWM voltage inverter are given in Fig. 7, which shows the total harmonic distortion of the output voltage of the two-level voltage inverter of 57.33 %.

Fig. 7 shows that the harmonics of the output voltage of the two-level inverter have higher harmonic frequencies multiple of the modulation frequency. The harmonic with the PWM frequency has the largest amplitude in the output voltage waveform, 32 % of the amplitude of the first harmonic of the output voltage. It should be noted that the relative value of the amplitudes of higher harmonics relative to the value of the first harmonic does not depend on the modulation frequency of the inverter [37, 38].

The LC filter is a second-order filter, the typical amplitude-frequency response (AFR) of which is shown in Fig. 8.

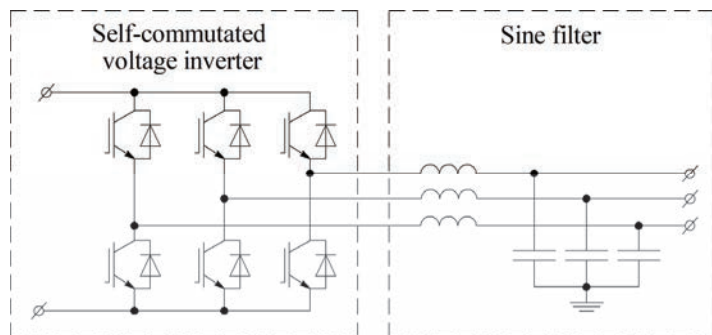


Fig. 6. Diagram of the two-level three-phase self-commutated voltage inverter with the sine filter

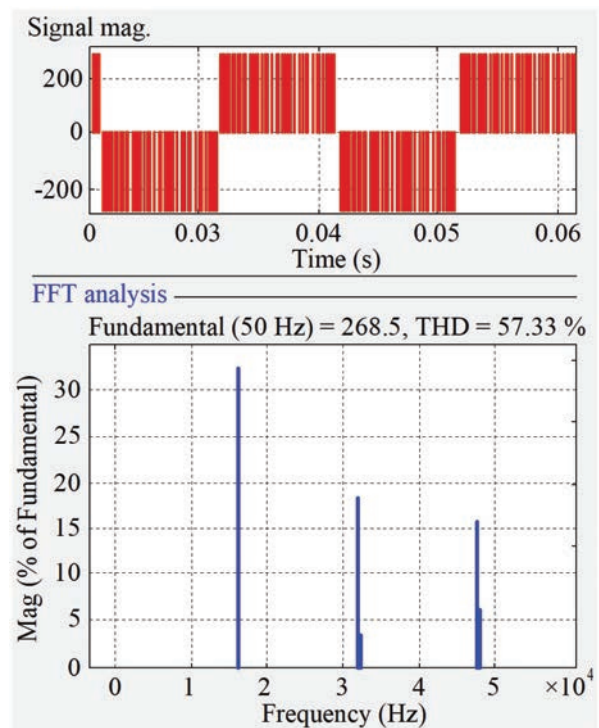


Fig. 7. Waveform and harmonic spectrum of the output voltage of the three-phase inverter

The resonant frequency of the LC filter is related to the filter values according to the expression:

$$F_C = \frac{1}{\pi\sqrt{LC}}. \tag{2}$$

To meet the requirements for the total harmonic distortion of the sine filter output voltage less than 5 %, the amplitudes of higher harmonics from the voltage inverter must be suppressed [39, 40]. The resonant frequency of the filter must be related to the modulation frequency of the inverter in two orders of magnitude:

$$f_C = \frac{F_{PWM}}{100}, \tag{3}$$

where  $f_C$  is the cutoff frequency of the LC filter,  $F_{PWM}$  is the PWM frequency in the self-commutated voltage inverter.

Thus, the parameters of the LC filter taking into account the PWM frequency can be calculated from the expression:

$$LC = \frac{1}{(\pi \cdot F_{PWM})^2}. \tag{4}$$

The study on the computer model has shown that at the moment of starting the self-commutated voltage inverter with the sine filter, when the filter capacitors are discharged, a transient process occurs. During this process, there is a significant increase in the current amplitude of the filter capacitors.

The amplitude of the starting current can be found through the value of the characteristic resistance of the filter, determined from the expression:

$$R_x = \sqrt{\frac{L}{C}}. \tag{5}$$

The amplitude of the starting current of the LC filter capacitor with the SCVI can be calculated from the expression:

$$I_{startC} = \frac{U_{DC}}{2,7 \cdot R_x}. \tag{6}$$

The magnitude of capacitor starting current is a significant limitation of the system, as it can lead to a failure of inverter power transistors. Therefore, when designing the sine filter, the value of the allowable inverter current  $I_{max}$  and the value of the current margin factor of power switches  $K_1$  must be taken into account. The starting current margin factor of the filter capacitor relative to the maximum inverter current is determined by:

$$K_1 = \frac{I_{max}}{I_{startC}}. \tag{7}$$

Thus, taking into account the modulation frequency of the voltage inverter, the requirements for limiting the allowable value of the filter capacitor starting current and the requirement to ensure the total harmonic distortion under the IEEE-519 standard, the inductance and capacitance of the sine filter can be determined by:

$$\frac{L}{C} = \left( \frac{U_{DC}}{2,7 \cdot I_{max} \cdot K_1} \right)^2; \tag{8}$$

$$LC = \frac{1}{(\pi \cdot F_{PWM})^2}. \tag{9}$$

We express the inductance and capacitance of the sine filter through equations (8), (9):

$$C = \sqrt{\frac{1}{(\pi \cdot F_{PWM})^2 \cdot \left( \frac{U_{DC}}{2,7 \cdot I_{max} \cdot K_1} \right)^2}}; \tag{10}$$

$$L = \sqrt{\frac{1}{(\pi \cdot F_{PWM})^2} \cdot \left( \frac{U_{DC}}{2,7 \cdot I_{max} \cdot K_1} \right)^2}, \tag{11}$$

where  $U_{DC}$  is the inverter DC voltage,  $I_{max}$  is the maximum allowable inverter current,  $K_1$  is the set current margin factor,  $F_{PWM}$  is the inverter PWM frequency.

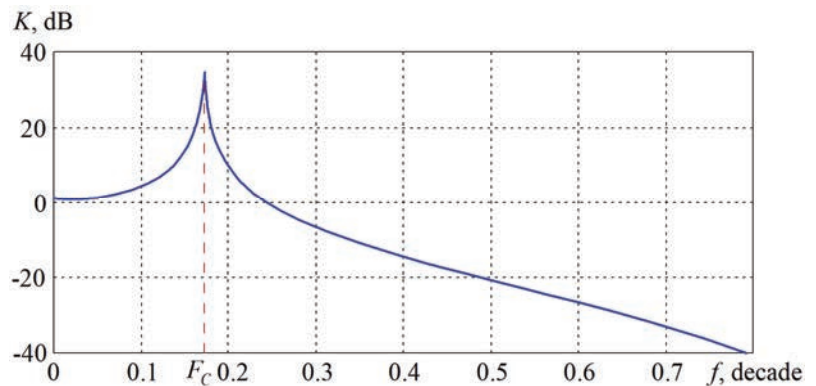


Fig. 8. Typical amplitude-frequency response of the LC filter ( $F_C$  – maximum peak resonant frequency)

### 6. Simulation of the three-phase two-level voltage inverter with the developed output sine filter

To confirm the generation of the sinusoidal waveform of the output voltage of the sine filter with  $THDU < 5\%$  and limitation of the starting current of the filter capacitors, a simulation model was developed in the Matlab/Simulink software environment. The developed simulation model for the studied system is shown in Fig. 9.

The parameters of the simulation model are given in Table 2.

Table 2

Simulation model parameters

Parameter	Value
Active load resistance, Ohms	40
Load inductance, mH	5
DC voltage, V	310
Sine filter inductance, mH	8; 4; 2; 1
Sine filter capacitance, uF	10; 20; 40; 80

Fig. 10 shows the waveform of the starting current of the sine filter capacitor at a filter inductance of 2 mH and capacitance of 40  $\mu$ F.

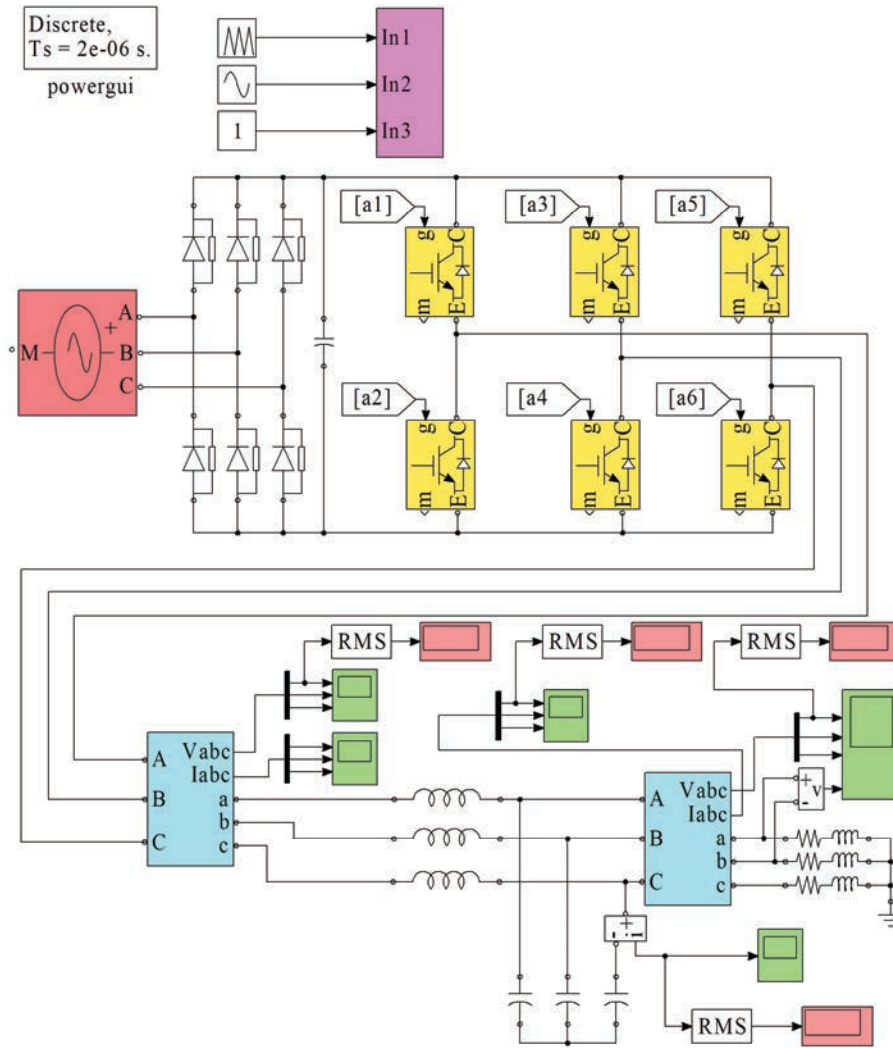


Fig. 9. Simulation model of the test bench

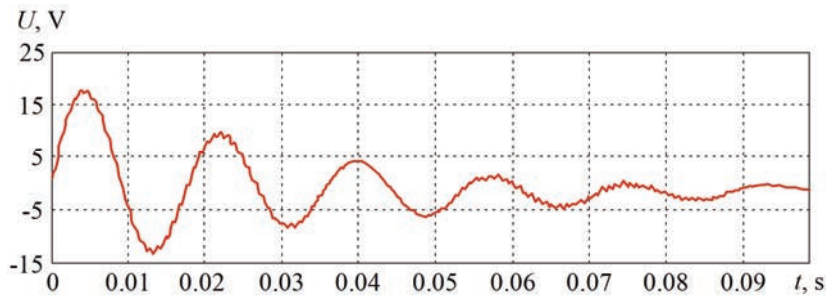


Fig. 10. Waveform of the starting current of the sine filter capacitor

Table 3 shows the capacitor starting current at 310 V DC voltage for different filter parameters.

Table 3

Starting current for different filter parameters

Filter characteristic impedance $R_p$ , Ohms	Filter inductance $L$ , mH	Filter capacitance $C$ , uF	Starting current peak amplitude by the simulation results $I_s$ , A
28,284	8	10	4
14,142	4	20	8
7,071	2	40	18
3,536	1	80	38

Fig. 11 shows the results of simulation of the frequency converter with the developed sine filter.

As can be seen from Fig. 11, the output voltage of the sine filter after the transient has an almost sinusoidal waveform.

The results of the harmonic analysis of the waveform of the sine filter output voltage are shown in Fig. 12.

As shown in Fig. 12, the output voltage of the sine filter has an almost sinusoidal waveform, and the total harmonic distortion is 1.88 %, which provides quality requirements for this waveform.

The reliability of the Matlab simulation results is confirmed using the method of solving ordinary differential equations ode23tb – the implicit Runge-Kutta method,

which uses second-order backward differentiation formulas. The simulation used a variable calculation step – a maximum sampling step of 1 μs and a minimum sampling step in time of 1 ns. The set value of the maximum allowable relative simulation error was 0.1 %.

the harmonics of the self-commutated voltage inverter, a physical bench was developed, which follows the diagram investigated on the simulation model in the Matlab/Simulink software environment. The diagram of the developed bench is given in Fig. 13.

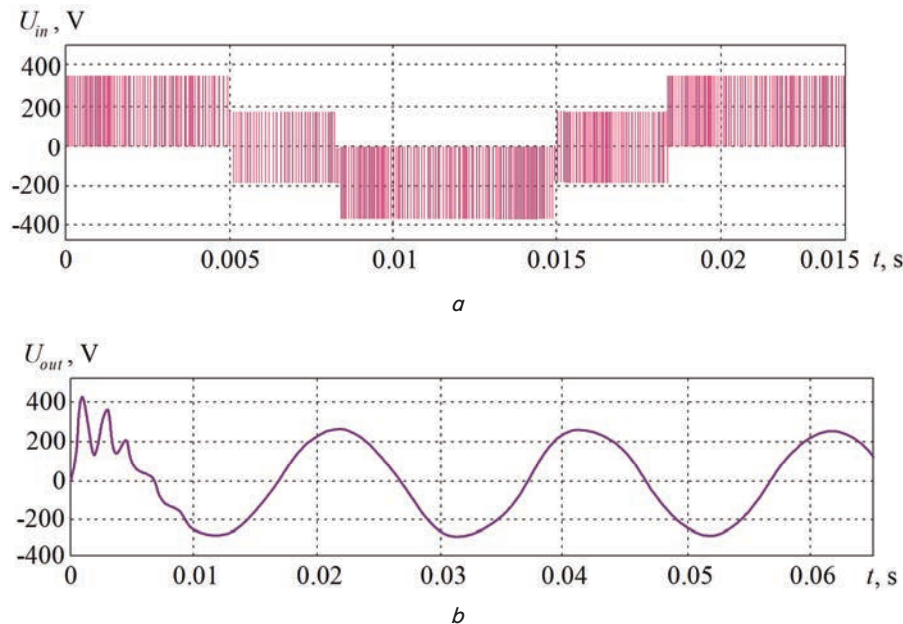


Fig. 11. Results of simulation: *a* – waveform of the output phase voltage of the sine filter; *b* – waveform of the output phase voltage of the sine filter

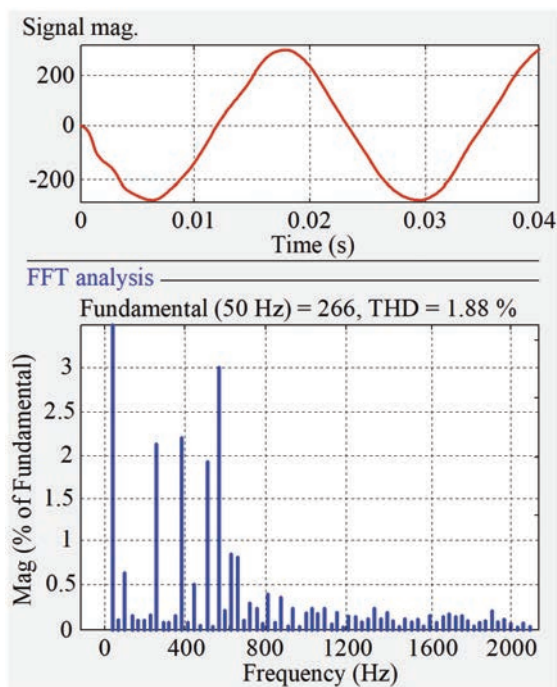


Fig. 12. Results of harmonic analysis of the sine filter output voltage

### 7. Study of the frequency converter sine filter operation on the physical bench

In order to confirm the generation of the sinusoidal waveform of the output voltage of the sine filter that filters

The developed bench (Fig. 14) used the PChV203-5K5-V frequency converter with a nominal power of 5.5 kW manufactured by OVEN, containing a three-phase diode rectifier, a DC link with an LC filter and a three-phase self-commutated voltage inverter. The frequency converter is set to a PWM frequency of 16 kHz. The sine filter uses JYUR phase-shifting capacitors with a capacity of 40 μF±5 and RMT-016-A power inductors with an inductance of 2.3 mH and RMT-004-A with an inductance of 0.46 mH manufactured by OVEN. During the study, two options for the bench load were tested:

1) 2A480V6PAU3 three-phase induction motor with a capacity of 1.5 kW, manufactured by LLC “Dnipropresurs” (Ukraine), which in the low torque mode causes a load current of 0.7–0.8 A (Fig. 13, *a*);

2) three wye-connected rheostats with a resistance of 40 Ohms each (Fig. 13, *b*).

The waveform and harmonic composition of the output linear voltage of the three-phase inverter were investigated using a SIGLENTSDS1104X-E oscilloscope, manufactured in China. The oscilloscope allows a harmonic analysis of the output voltage waveform, but does not determine the integral value of total harmonic distortion. The basic oscilloscope parameters are given in Table 4.

Table 4

Basic parameters of the SIGLENTSDS1104X-E oscilloscope

Parameter	Value
Bandwidth	100 MHz
Sampling rate	1 GHz
Oscillogram capture rate	400,000 osc/sec
Vertical permissible measurement error	500 μV/division

The amplitude-frequency response of the oscilloscope measuring channel is shown in Fig. 15.

According to the amplitude-frequency response of the input channel, the cutoff frequency is 18 MHz.

The oscillograms of the output linear voltage of the frequency converter without filtering and its spectral analysis – the results of fast Fourier transform – are shown in Fig. 16.

As can be seen from Fig. 16, the output voltage spectrum contains harmonics multiple of the PWM frequency, i.e. 16 kHz, 32 kHz, 48 kHz, etc.

The studies show that the type of load (resistive-inductive or resistive) does not significantly affect the sinusoidality of the sine filter output voltage waveform. The waveform of the output voltage of the sine filter and its spectral analysis (fast Fourier transform) are shown in Fig. 17.

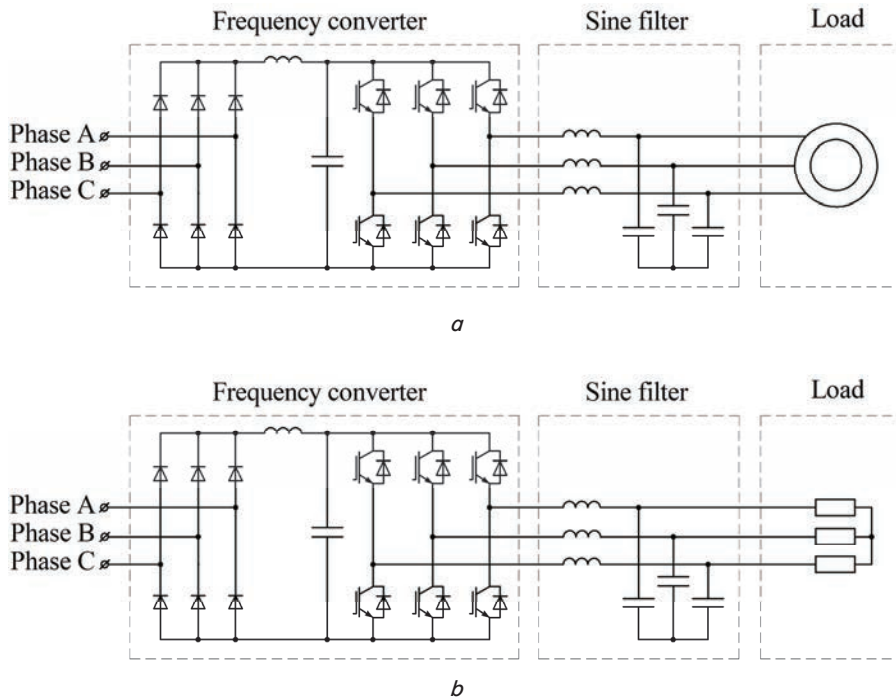


Fig. 13. Power circuit of the developed bench: *a* – bench load is a three-phase induction motor; *b* – bench load is three wye-connected rheostats

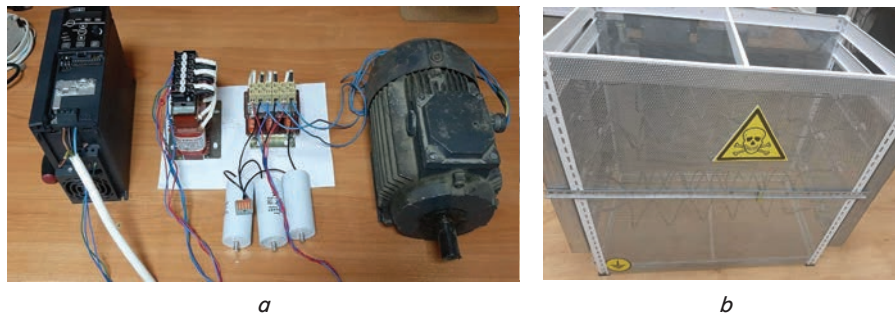


Fig. 14. Photo of the developed bench of the frequency converter and sine filter: *a* – bench load is a three-phase induction motor; *b* – bench load is three wye-connected rheostats

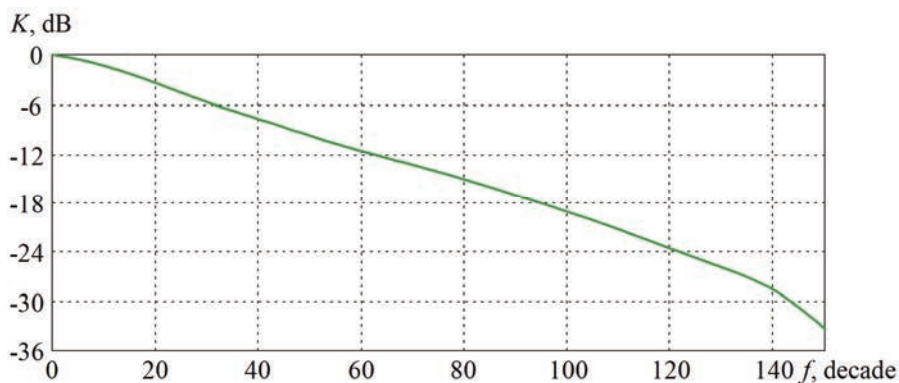


Fig. 15. Amplitude-frequency response of the bandwidth of the SIGLENTSDS1104X-E oscilloscope measuring channel

As can be seen from Fig. 17, the filtering of the output voltage of the frequency converter proved to be quite effective and provides the generated voltage of the sinusoidal waveform. In this case, the higher harmonics of the output voltage of the frequency converter associated with the switching frequency are quite small and lie within 1–2 V.

The starting current modes of the PChV203-5K5-V frequency converter for different configurations of filter induc-

tance were also investigated on the developed bench. During the experiment, RMT-004-A power inductors with an inductance of 0.4 mH and a capacitance of 40  $\mu$ F ( $R_x=3.162$  Ohm,  $I_{start}=36$  A) were used. The frequency converter entered the protection mode at a maximum current of 20 A and turned off at startup. To ensure the normal functional mode of the bench, a series connection of two RMT-016-A inductors with a total inductance of 4.6 mH and a capacity of 40  $\mu$ F ( $R_x=10.7$  Ohm,



$I_{start}=10.7\text{ A}$ ) was used, after which the starting current did not exceed the PChV203-5K5-V protection current of 20 A.



Fig. 16. Oscillograms of the output linear voltage of the frequency converter before filtering and its spectral analysis (fast Fourier transform): *a* – the load is a three-phase induction motor; *b* – the load is three wye-connected rheostats



Fig. 17. Waveform of the output phase voltage of the frequency converter and its spectral analysis (fast Fourier transform): *a* – the load is a three-phase induction motor; *b* – the load is three wye-connected rheostats

Comparison of the results of simulation and physical experiment is given in Table 5.

Table 5

Comparison of simulation and physical experiment results

Parameter	Simulation results	Physical experiment results
Harmonic frequencies in the output voltage spectrum of the self-commutated inverter	16 kHz, 32 kHz, 48 kHz, ...	16 kHz, 32 kHz, 48 kHz, ...
Waveform and THD of the output voltage of the self-commutated voltage inverter	Pulse waveform, THD=57.33 %	Pulse waveform, THD=59.72 %
Waveform and THD of the output voltage of the sine filter	Sinusoidal waveform, THD=1.88 %	Sinusoidal waveform, THD=2.56 %
Checking the starting current limitation of the sine filter capacitor by (6)–(11)	Performed by the criterion of obtaining the capacitor starting current oscillogram	Performed by the criterion of switching off the frequency converter at maximum current

As can be seen from Table 5, the results of the simulation and physical experiment generally coincide, but the physical experiment revealed an increased value of higher harmonics, so the THD values of the voltage inverter and the sine filter are slightly higher. This can be justified by the fact that in real conditions there are induction of the measuring channel, harmonics from the mains and error

of the measuring channel. Despite this, the obtained value of the total harmonic distortion of the output voltage of the developed sine filter does not exceed 5 % and meets the voltage quality requirements under the international standard IEEE-519.

**8. Discussion of the results of the study of improving the output voltage quality of two-level self-commutated voltage inverters with sine filters**

The developed method of calculating the parameters of the sine filter of the two-level voltage inverter in the PWM mode is presented. A feature of the method – equations (8), (9) – is the determination of the filter parameters that provide the sinusoidality of the output voltage  $THD_U < 5\%$ , taking into account the PWM frequency of the voltage inverter and the requirements of limiting the starting current of the filter capacitor.

In the Matlab/Simulink computer simulation system, the process of increasing the sinusoidality of the output voltage of the frequency converter with the

developed sine filter was investigated (Fig 9–12). The studies confirmed the provision of the desired sinusoidality of the filter output voltage with the total harmonic distortion of 1.88 % (Fig. 12) and the dependence of the starting current on the filter parameters (Table 3).

A physical prototype of the investigated system was developed based on the 5.5 kW OVEN PChV203-5K5-V frequency converter, 40  $\mu\text{F}$  phase-shifting capacitors, 2.3 mH RMT-016-A inductors and 0.46 mH RMT-004-A. As the bench load, in the first case, a 2A480V6PAU3 three-phase induction motor was used (Fig. 13, *a*), in the second case – three wye-connected rheostats (Fig. 13, *b*). On the developed bench, the process of increasing the sinusoidality of the output voltage by spectral analysis was studied (Fig. 16, 17), as well as the limitation of the start of the frequency converter by the maximum starting current.

The limitation of the study is that the developed simulation model works adequately only in operating modes, and emergency modes, in which the voltage and current values exceed the rated values, will be reflected inadequately.

The disadvantage of the proposed solution to provide the sinusoidal voltage of the two-level voltage inverter with the LC filter is a significant voltage drop across the filter inductor, which causes the non-use of DC link voltage.

A possible direction for further development of the research is the study of filters of other topologies in order to reduce the voltage drop across the filter, as well as the creation of multi-level inverters with a reduced number of power transistors.

The developed method of calculating the values of the sine filter of the frequency converter is used in the design office of LLC “VO OVEN” (Ukraine).

## 9. Conclusions

1. Analytical dependences of the values of the sine filter of the two-level voltage inverter in the PWM mode, which provides, firstly, the sinusoidality of the output voltage under the international standard IEEE-519 taking into account the PWM frequency of the voltage inverter, and, secondly, limitation of the starting current to the required value, were developed.

2. In the Matlab 2017b software environment, the simulation model of the frequency converter with the sine filter was developed. The studies confirmed the limitation of the starting current of the sine filter capacitor. In addition, the studies showed the total harmonic distortion of the output phase voltage of 1.88 % after filtration, which

meets the power quality requirements of international standards.

3. The physical model of the studied system was developed. The physical prototype based on the 5.5 kW PChV203-5K5-V three-phase frequency converter, set to a PWM frequency of 16 kHz, the sine filter and the filter load – the 2A480V6PAU3 three-phase induction motor or three wye-connected rheostats was developed. Oscillograms of the output voltages of the frequency converter and the sine filter were obtained. A harmonic Fourier analysis of the obtained oscillograms was performed. The proposed method of calculating the parameters of the sine filter that implements the sinusoidal waveform of the output voltage was confirmed on the simulation model and the physical bench.

## References

1. Brynolf, S., Taljegard, M., Grahn, M., Hansson, J. (2018). Electrofuels for the transport sector: A review of production costs. *Renewable and Sustainable Energy Reviews*, 81 (2), 1887–1905. doi: <http://doi.org/10.1016/j.rser.2017.05.288>
2. Capellán-Pérez, I., de Castro, C., Arto, I. (2017). Assessing vulnerabilities and limits in the transition to renewable energies: Land requirements under 100% solar energy scenarios. *Renewable and Sustainable Energy Reviews*, 77, 760–782. doi: <https://doi.org/10.1016/j.rser.2017.03.137>
3. Miller, L. M., Keith, D. W. (2018). Observation-based solar and wind power capacity factors and power densities. *Environmental Research Letters*, 13 (10). doi: <http://doi.org/10.1088/1748-9326/aae102>
4. Moran, E. F., Lopez, M. C., Moore, N., Muller, N., Hyndman, D. W. (2018). Sustainable hydropower in the 21st century. *PNAS*, 115 (47), 11891–11898. doi: <http://doi.org/10.1073/pnas.1809426115>
5. Raugei, M., Sgouridis, S., Murphy, D. et. al. (2017). Energy Return on Energy Invested (ERoEI) for photovoltaic solar systems in regions of moderate insolation: A comprehensive response. *Energy Policy*, 102, 377–384. doi: <http://doi.org/10.1016/j.enpol.2016.12.042>
6. Ferroni, F., Guekos, A., Hopkirk, R. J. (2017). Further considerations to: Energy Return on Energy Invested (ERoEI) for photovoltaic solar systems in regions of moderate insolation. *Energy Policy*, 107, 498–505. doi: <https://doi.org/10.1016/j.enpol.2017.05.007>
7. Ansell, T., Cayzer, S. (2018). Limits to growth redux: A system dynamics model for assessing energy and climate change constraints to global growth. *Energy Policy*, 120, 514–525. doi: <https://doi.org/10.1016/j.enpol.2018.05.053>
8. Plakhtii, O. A., Nerubatskyi, V. P., Hordiienko, D. A., Tsybulnyk, V. R. (2019). Analysis of the energy efficiency of a two-level voltage source inverter in the overmodulation mode. *Naukovyi Visnyk Natsionalnoho Hirnychoho Universytetu*, 4 (172), 68–72. doi: <http://doi.org/10.29202/nvngu/2019-4/9>
9. Plakhtii, O., Nerubatskyi, V., Karpenko, N., Ananieva, O., Khoruzhevskyi, H., Kavun, V. (2019). Studying a voltage stabilization algorithm in the cells of a modular sixlevel inverter. *Eastern-European Journal of Enterprise Technologies*, 6 (8 (102)), 19–27. doi: <https://doi.org/10.15587/1729-4061.2019.185404>
10. Plakhtii, O. A., Nerubatskyi, V. P., Kavun, V. Y., Hordiienko, D. A. (2019). Active single-phase four-quadrant rectifier with improved hysteresis modulation algorithm. *Naukovyi Visnyk Natsionalnoho Hirnychoho Universytetu*, 5, 93–98. doi: <https://doi.org/10.29202/nvngu/2019-5/16>
11. Chaurasia, G. S., Singh, A. K., Agrawal, S., Sharma, N. K. (2017). A meta-heuristic firefly algorithm based smart control strategy and analysis of a grid connected hybrid photovoltaic/wind distributed generation system. *Solar Energy*, 150, 265–274. doi: <https://doi.org/10.1016/j.solener.2017.03.079>
12. Plakhtii, O., Nerubatskyi, V., Scherbak, Ya., Mashura, A., Khomenko, I. (2020). Energy efficiency criterion of power active filter in a three-phase network. *2020 IEEE KhPI Week on Advanced Technology (KhPIWeek)*, 165–170. doi: <https://doi.org/10.1109/KhPIWeek51551.2020.9250073>
13. Priyan, S. S., Ramani, K. (2013). Implementation of closed loop system for flying capacitor multilevel inverter with stand-alone Photovoltaic input. *2013 International Conference on Power, Energy and Control (ICPEC)*. doi: <https://doi.org/10.1109/icpec.2013.6527666>
14. Chen, W., Sun, H., Gu, X., Xia, C. (2016). Synchronized Space-Vector PWM for Three-Level VSI With Lower Harmonic Distortion and Switching Frequency. *IEEE Transactions on Power Electronics*, 31 (9), 6428–6441. doi: <https://doi.org/10.1109/tpel.2015.2499774>
15. Plakhtii, O., Nerubatskyi, V., Khomenko, I., Tsybulnyk, V., Syniavskyi, A. (2020). Comprehensive Study Of Cascade Multilevel Inverters With Three Level Cells. *2020 IEEE 7th International Conference on Energy Smart Systems (ESS)*. doi: <https://doi.org/10.1109/ess50319.2020.9160258>
16. Kumari, B., Sankar, M. (2014). Modeling and individual voltage balancing control of modular multilevel cascade converter. *International Journal of Emerging Engineering Research and Technology*, 2 (1), 42–48.
17. Sokol, Y., Ivakhno, V., Zamaruev, V., Styslo, B. (2018). Full Soft Switching Dual DC/DC Converter With Four-Quadrant Switch for Systems With Battery Energy Storage System. *2018 IEEE 3rd International Conference on Intelligent Energy and Power Systems (IEPS)*. doi: <https://doi.org/10.1109/ieps.2018.8559490>

18. Maurya, S., Mishra, D., Singh, K., Mishra, A. K., Pandey, Y. (2019). An Efficient Technique to reduce Total Harmonics Distortion in Cascaded H- Bridge Multilevel Inverter. 2019 IEEE International Conference on Electrical, Computer and Communication Technologies (ICECCT). doi: <https://doi.org/10.1109/icecct.2019.8869424>
19. Martinez-Rodrigo, F., Ramirez, D., Rey-Boue, A., de Pablo, S., Herrero-de Lucas, L. (2017). Modular Multilevel Converters: Control and Applications. *Energies*, 10 (11), 1709. doi: <https://doi.org/10.3390/en10111709>
20. Gervasio, F., Mastromauro, R. A., Liserre, M. (2015). Power losses analysis of two-levels and three-levels PWM inverters handling reactive power. 2015 IEEE International Conference on Industrial Technology (ICIT). doi: <https://doi.org/10.1109/icit.2015.7125248>
21. Ganesh, P., Shanmugavadivu, N., Santha, K. (2018). Single-Phase 63-Level Modular Multilevel Inverter fed Induction Motor Drive for Solar PV Applications. 2018 4th International Conference on Electrical Energy Systems (ICEES). doi: <https://doi.org/10.1109/icees.2018.8443287>
22. Kumar, S. S., Sasikumar, M. (2016). An approach of hybrid modulation in fusion seven-level cascaded multilevel inverter accomplishment to IM drive system. 2016 Second International Conference on Science Technology Engineering and Management (ICONSTEM). doi: <https://doi.org/10.1109/iconstem.2016.7560980>
23. Ahmadzadeh, T., Sabahi, M., Babaei, E. (2017). Modified PWM control method for neutral point clamped multilevel inverters. 2017 14th International Conference on Electrical Engineering/Electronics, Computer, Telecommunications and Information Technology (ECTI-CON). doi: <https://doi.org/10.1109/ecticon.2017.8096351>
24. Plakhtii, O., Tsybulnyk, V., Nerubatskyi, V., Mittsel, N. (2019). The Analysis Of Modulation Algorithms and Electromagnetic Processes in a Five-Level Voltage Source Inverter with Clamping Diodes. 2019 IEEE International Conference on Modern Electrical and Energy Systems (MEES). doi: <https://doi.org/10.1109/mees.2019.8896567>
25. Ahmed, B., Aganah, K. A., Ndoeye, M., Arif, M. A., Luciano, C., Murphy, G. V. (2017). Single-phase cascaded multilevel inverter topology for distributed DC sources. 2017 IEEE 8th Annual Ubiquitous Computing, Electronics and Mobile Communication Conference (UEMCON). doi: <https://doi.org/10.1109/uemcon.2017.8248980>
26. Rajesh, B., Manjesh. (2016). Comparison of harmonics and THD suppression with three and 5 level multilevel inverter-cascaded H-bridge. 2016 International Conference on Circuit, Power and Computing Technologies (ICCPCT). doi: <https://doi.org/10.1109/iccpct.2016.7530116>
27. Piao, C., Hung, J. Y. (2015). A novel SVPWM overmodulation technique for three-level NPC VSI. 2015 IEEE Transportation Electrification Conference and Expo (ITEC). doi: <https://doi.org/10.1109/itec.2015.7165744>
28. Raval, K. Y., Ruvavara, V. J. (2018). Novel Multilevel Inverter Design with Reduced Device Count. 2018 International Conference on Current Trends Towards Converging Technologies (ICCTCT). doi: <https://doi.org/10.1109/icctct.2018.8550867>
29. Gupta, K. K., Jain, S. (2013). A multilevel Voltage Source Inverter (VSI) to maximize the number of levels in output waveform. *International Journal of Electrical Power & Energy Systems*, 44 (1), 25–36. doi: <https://doi.org/10.1016/j.ijepes.2012.07.008>
30. Tugay, D., Korneliuk, S., Akymov, V., Zhemerov, G. (2020). Localization of the Phase Voltage Measurement Location for Active Power Filter Controlling. 2020 IEEE 4th International Conference on Intelligent Energy and Power Systems (IEPS). doi: <https://doi.org/10.1109/ieps51250.2020.9263137>
31. Todkar, R. R., Shinde, S. M. (2016). A Solar Photovoltaic system for ATM by using Buck-Boost Integrated Full Bridge Inverter. 2016 2nd International Conference on Advances in Electrical, Electronics, Information, Communication and Bio-Informatics (AEEICB). doi: <https://doi.org/10.1109/aeecb.2016.7538304>
32. Vdovin, V. V., Kotin, D. A., Pankratov, V. V. (2014). Parameters determination in the sine filters for AFE converters and VSI with PWM. 2014 15th International Conference of Young Specialists on Micro/Nanotechnologies and Electron Devices (EDM). doi: <https://doi.org/10.1109/edm.2014.6882553>
33. Kurwale, M. V., Sharma, P. G., Bacher, G. (2014). Performance analysis of modular multilevel converter (MMC) with continuous and discontinuous pulse width modulation (PWM). *International Journal of Advanced Research in Electrical, Electronics and Instrumentation Engineering*, 3 (2), 7463–7474.
34. Schobre, T., Mallwitz, R. (2020). Automated Design Method for Sine Wave Filters in Motor Drive Applications with SiC-Inverters. 2020 22nd European Conference on Power Electronics and Applications (EPE'20 ECCE Europe). doi: <https://doi.org/10.23919/epe20ecceurope43536.2020.9215952>
35. Scherback, Y. V., Plakhtiy, O. A., Nerubatskiy, V. P. (2017). Control characteristics of active four-quadrant converter in rectifier and recovery mode. *Tekhnichna Elektrodynamika*, 6, 26–31. doi: <https://doi.org/10.15407/techned2017.06.026>
36. Plakhtii, O., Nerubatskyi, V., Sushko, D., Hordiienko, D., Khoruzhevskiy, H. (2020). Improving the harmonic composition of output voltage in multilevel inverters under an optimum mode of amplitude modulation. *Eastern-European Journal of Enterprise Technologies*, 2 (8 (104)), 17–24. doi: <https://doi.org/10.15587/1729-4061.2020.200021>
37. Tugay, D., Kolontaievskiy, Y., Korneliuk, S., Akymov, V. (2020). Comparison of the compensation quality for active power filter control techniques. 2020 IEEE KhPI Week on Advanced Technology (KhPIWeek), 236–241. doi: <https://doi.org/10.1109/KhPIWeek51551.2020.9250092>
38. Zhemerov, G., Iliina, N., Tugay, D. (2016). The theorem of minimum energy losses in three-phase four-wire energy supply system. 2016 2nd International Conference on Intelligent Energy and Power Systems (IEPS). doi: <https://doi.org/10.1109/ieps.2016.7521889>
39. Mao, C., Zhu, Y., Li, Z., Ming, X. (2018). Design of LC bandpass filters based on silicon-based IPD Technology. 2018 19th International Conference on Electronic Packaging Technology (ICEPT). doi: <https://doi.org/10.1109/icept.2018.8480419>
40. Munjer, M. A., Sheikh, M. R. I., Alim, M. A., Boddapati, V., Musib, M. A. (2018). Minimization of THD for Multilevel Converters with triangular injection approach. 2018 3rd International Conference for Convergence in Technology (I2CT). doi: <https://doi.org/10.1109/i2ct.2018.8529750>